SUPPLEMENTARY INFORMATION

MODELING BIOFILMS WITH DUAL EXTRACELLULAR ELECTRON TRANSFER MECHANISMS

Ryan Renslow[1†], Jerome Babauta[1], Andrew Kuprat[2], Jim Schenk[3#], Cornelius Ivory[1], Jim Fredrickson[4], and Haluk Beyenal[1*]

[1] The Gene and Linda Voiland School of Chemical Engineering and Bioengineering, Washington State University, Pullman, WA, United States of America
[2] Fundamental and Computational Sciences Directorate, Pacific Northwest National Laboratory, Richland, WA, United States of America
[3] The Department of Chemistry, Washington State University, Pullman, WA, United States of America
[4] Biological Sciences Division, Pacific Northwest National Laboratory, Richland, Washington 99352, United States of America

[†] Current address: Environmental Molecular Sciences Laboratory, Pacific Northwest National Laboratory, Richland, WA, United States of America.

[#] In memory of our collaborator and friend James "Jim" O. Schenk (August 30, 1952—January 31, 2013). We are grateful for his significant contribution to this paper.

[*] Corresponding author. Mailing address: The Gene and Linda Voiland School of Chemical Engineering and Bioengineering, Washington State University, 118 Dana Hall Spokane St., P.O. Box 642710, Pullman, WA 99164-2710. Phone: (509) 335-6607, Fax: (509) 335-4806.

I. MODEL SYSTEM OF EQUATIONS

The model consists of a set of four second-order differential equations. The four dependent variables are substrate, S; oxidized mediator, M_o; reduced mediator, M_r; and biofilm matrix potential, E. Below are all of the differential equations, initial conditions, and boundary conditions. Each boundary condition is specified as either a Dirichlet (first-type) or a Neumann (second-type) boundary condition. The electrode surface is at x = 0, and the top of the biofilm is at x = L.

Substrate mass balance

$$\frac{\partial S}{\partial t} = \frac{\partial}{\partial x}\left(D_{eS}\frac{\partial S}{\partial x}\right) - R_S$$

Initial Condition:	$S(t=0) = S(bulk)$	Biofilm is saturated
Boundary Condition 1:	$\frac{\partial S}{\partial x}(x=0) = 0$	Neumann BC (No flux at electrode)
Boundary Condition 2:	$S(x=L) = S(bulk)$	Dirichlet BC (Defined concentration)

Oxidized mediator mass balance

$$\frac{\partial M_o}{\partial t} = \frac{\partial}{\partial x}\left(D_{eM}\frac{\partial M_o}{\partial x}\right) - R_M$$

Initial Condition:	$M_o(t=0) = 0$	All mediators are reduced in biofilm
Boundary Condition 1:	$\frac{\partial M_o}{\partial x}(x=0) = -\frac{1}{D_{eM}}(r_o - r_r)$	Neumann BC (Butler-Volmer flux at electrode)
Boundary Condition 2:	$M_o(x=L) = M_o(bulk)$	Dirichlet BC (Defined concentration)

Reduced mediator mass balance

$$\frac{\partial M_r}{\partial t} = \frac{\partial}{\partial x}\left(D_{eM}\frac{\partial M_r}{\partial x}\right) + R_M$$

Initial Condition:	$M_r(t=0) = M_o(bulk)$	Equivalent concentration to bulk
Boundary Condition 1:	$\frac{\partial M_r}{\partial x}(x=0) = -\frac{1}{D_{eM}}(r_r - r_o)$	Neumann BC (Butler-Volmer flux at electrode)
Boundary Condition 2:	$M_r(x=L) = 0$	Dirichlet BC (Defined concentration)

Electron balance

$$\frac{\partial j_C}{\partial x} = -\frac{\partial}{\partial x}\left(\kappa\frac{\partial E}{\partial x}\right)$$

Initial Condition:	$E(t=0) = \varepsilon$	Biofilm has same potential as electrode
Boundary Condition 1:	$E(x=0) = \varepsilon$	Dirichlet BC (Defined potential at electrode)
Boundary Condition 2:	$\frac{\partial E}{\partial x}(x=L) = 0$	Neumann BC (No electrons out of top of biofilm)

Below are the relevant algebraic and differential expressions used in the four second-order differential equations:

Substrate Utilization

Specific substrate utilization via diffusion-based EET $q_M = q_{max}\left(\frac{S}{S+K_S}\right)\left(\frac{M_o}{M_o+K_M}\right)$

Specific substrate utilization via conduction-based EET $q_C = q_{max}\left(\frac{S}{S+K_S}\right)\left(\frac{1}{1+exp\left(-\frac{F}{\mathcal{R}T}\left(E-E_{K_A}\right)\right)}\right)$

Modified specific substrate utilization via diffusion-based EET

$$q_M^* \equiv f(q_C, q_M, q_{max}) = \begin{cases} q_M, & if\ \ q_M + q_C \le q_{max}\left(\frac{S}{S+K_S}\right) \\ q_{max}\left(\frac{S}{S+K_S}\right)\frac{q_M}{q_M+q_C}, & if\ \ q_M + q_C > q_{max}\left(\frac{S}{S+K_S}\right) \end{cases}$$

Modified specific substrate utilization via conduction-based EET

$$q_C^* \equiv f(q_C, q_M, q_{max}) = \begin{cases} q_C, & if\ \ q_M + q_C \le q_{max}\left(\frac{S}{S+K_S}\right) \\ q_{max}\left(\frac{S}{S+K_S}\right)\frac{q_C}{q_M+q_C}, & if\ \ q_M + q_C > q_{max}\left(\frac{S}{S+K_S}\right) \end{cases}$$

Reactions in the Biofilm Volume

Overall substrate consumption rate: $R_S = Xq = X(q_M^* + q_C^*)$

Reduction rate of M_o in the biofilm: $R_M = \frac{yf}{n} X q_M^*$

Generation rate of e^- in the biofilm: $R_C = yfX q_C^*$

Reactions at the Electrode Surface

Oxidation rate of M_r at the electrode surface $r_o = M_r k_0 e^{\left[(1-\alpha)\frac{nF}{\mathcal{R}T}(\epsilon - E_0)\right]}$

Reduction rate of M_o at the electrode surface $r_r = M_o k_0 e^{\left[-\alpha\frac{nF}{\mathcal{R}T}(\epsilon - E_0)\right]}$

Generation rate of e^- at the electrode surface $r_M = n(r_o - r_r)$

Current

Current produced by diffusion-based EET $j_M = F \cdot r_M$

Current produced by conduction-based EET $\nabla j_C = F \cdot R_C$ with $j_C(x = L) = 0$

Total current $j = j_M + j_C$

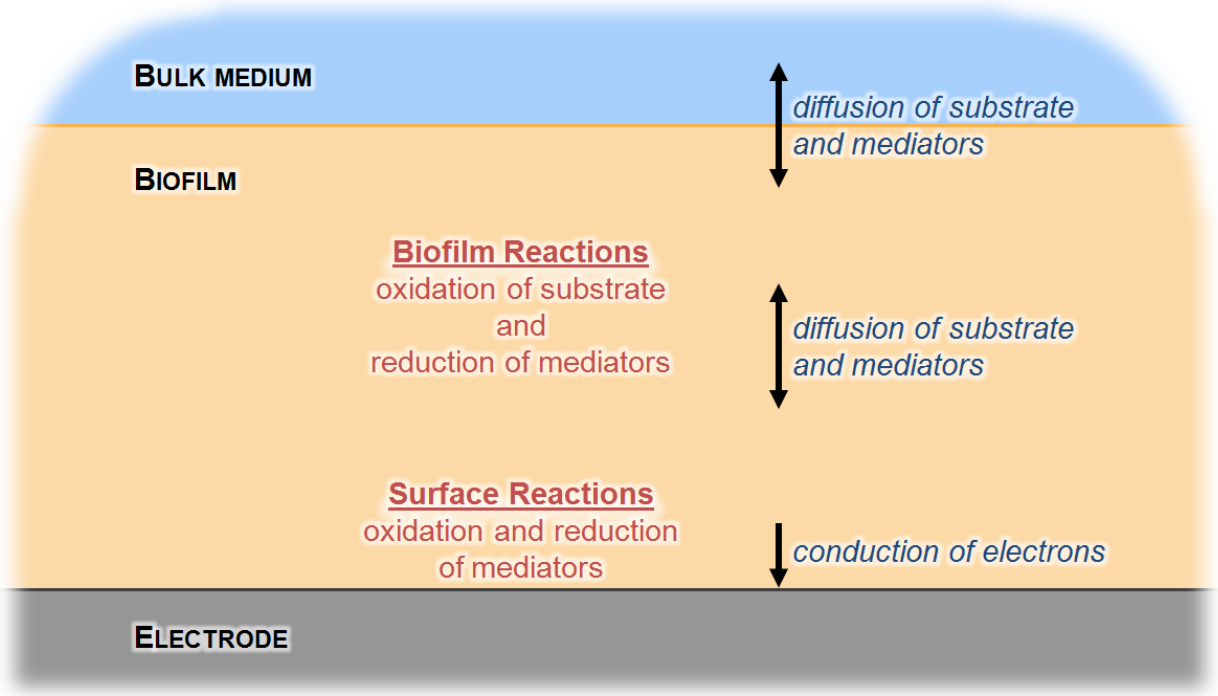

Figure S1. Schematic representation of the model standard case. The model considers a single domain, the biofilm, with two interfaces, the bulk medium at the top of the biofilm and the solid conducting electrode at the base of the biofilm.

II. Steady State Solution Convergence

We tested how model parameters converged to a steady state when the electrode potential was held constant (Figure S2).

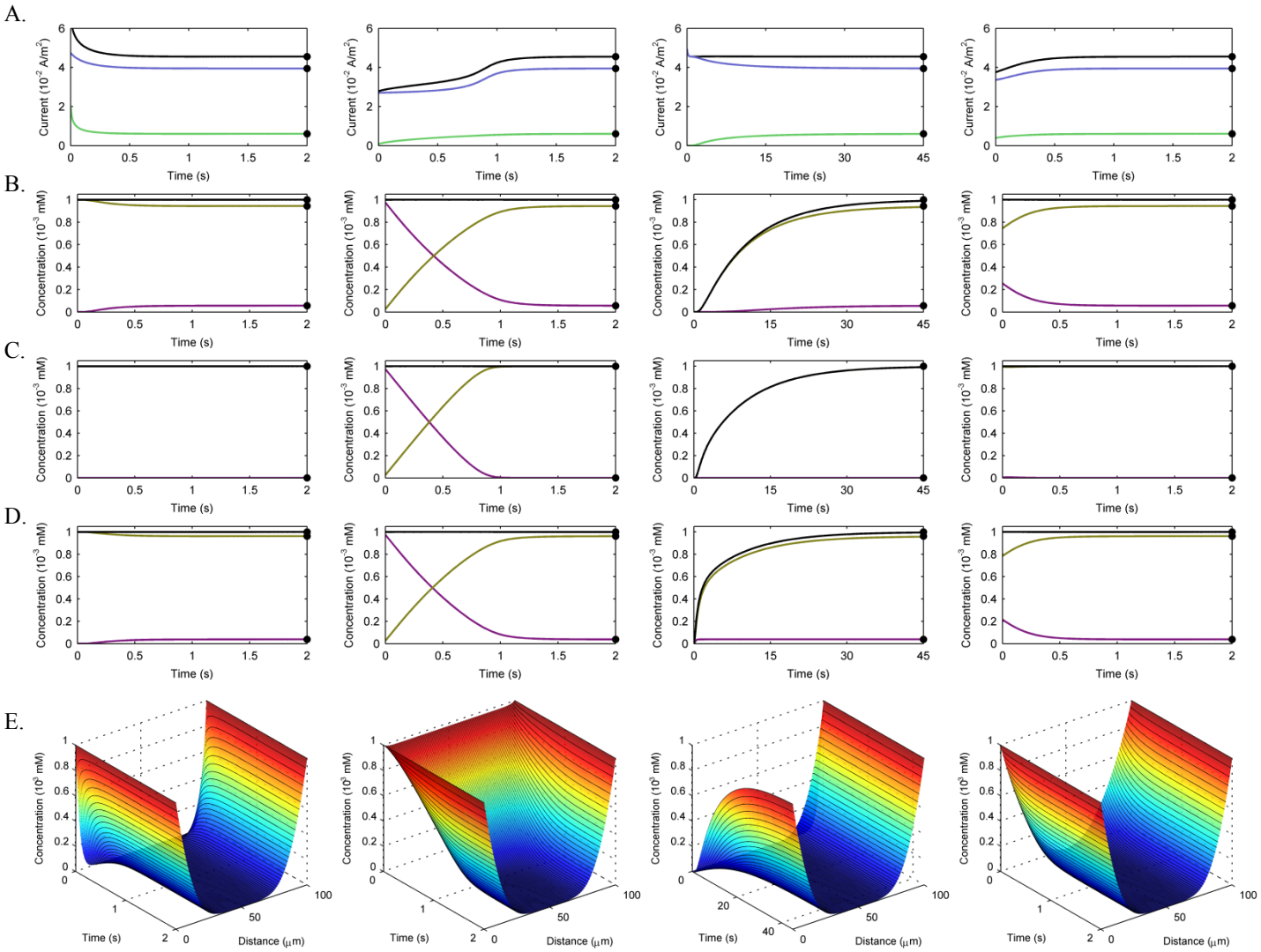

Figure S2. Convergence of a steady state solution for multiple initial conditions. The left column shows the convergence of several parameters for the model as described in the manuscript text and in the Model System of Equations in the Supplementary Information. The next column shows the convergence when the initial conditions are altered so that the mediator is 100% oxidized in the biofilm as opposed to 100% reduced. The second to last column shows the convergence when the initial conditions are altered so that the mediator concentration is zero inside the biofilm (i.e., mediators must diffuse in from the bulk over time). The last column shows the convergence when the initial conditions are altered so that the mediator concentration follows a parabolic profile, with all mediators oxidized at the biofilm-electrode and biofilm-solution interfaces and all mediators reduced in the middle of the biofilm.

A) Current via diffusion-based EET, green; current via conduction-based EET, blue; and total current, black. B) At 25 μm above the electrode: oxidized mediator concentration, purple; reduced mediator concentration, yellow; and total mediator concentration, black. C) At 50 μm. D) At 75 μm. Black solid dots mark the true steady state solutions. E) 3D plots showing convergence of the oxidized mediator concentration profile inside the biofilm over time (a 3D representation of the data presented in B, C, and D plots).

These results confirm 1) that the model solution converges smoothly with time, 2) that the final solution is independent of the initial condition of the mediators, and 3) the total mediator concentration is truly conserved.

III. PARAMETER ANALYSIS

We tested how model parameters affected both the current production and the percent of current due to diffusion- and conduction-based EET mechanisms. The results are shown in Figure S3.

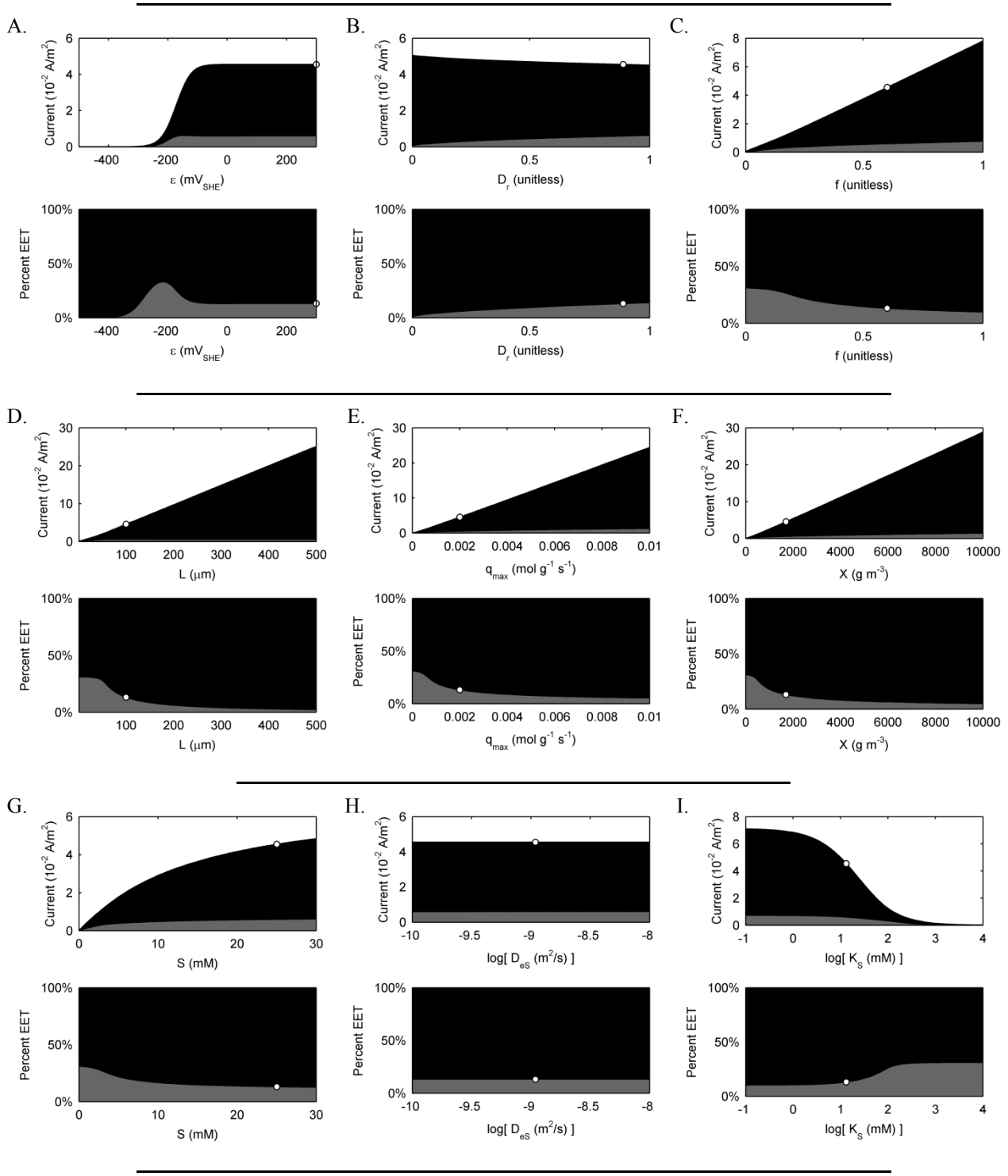

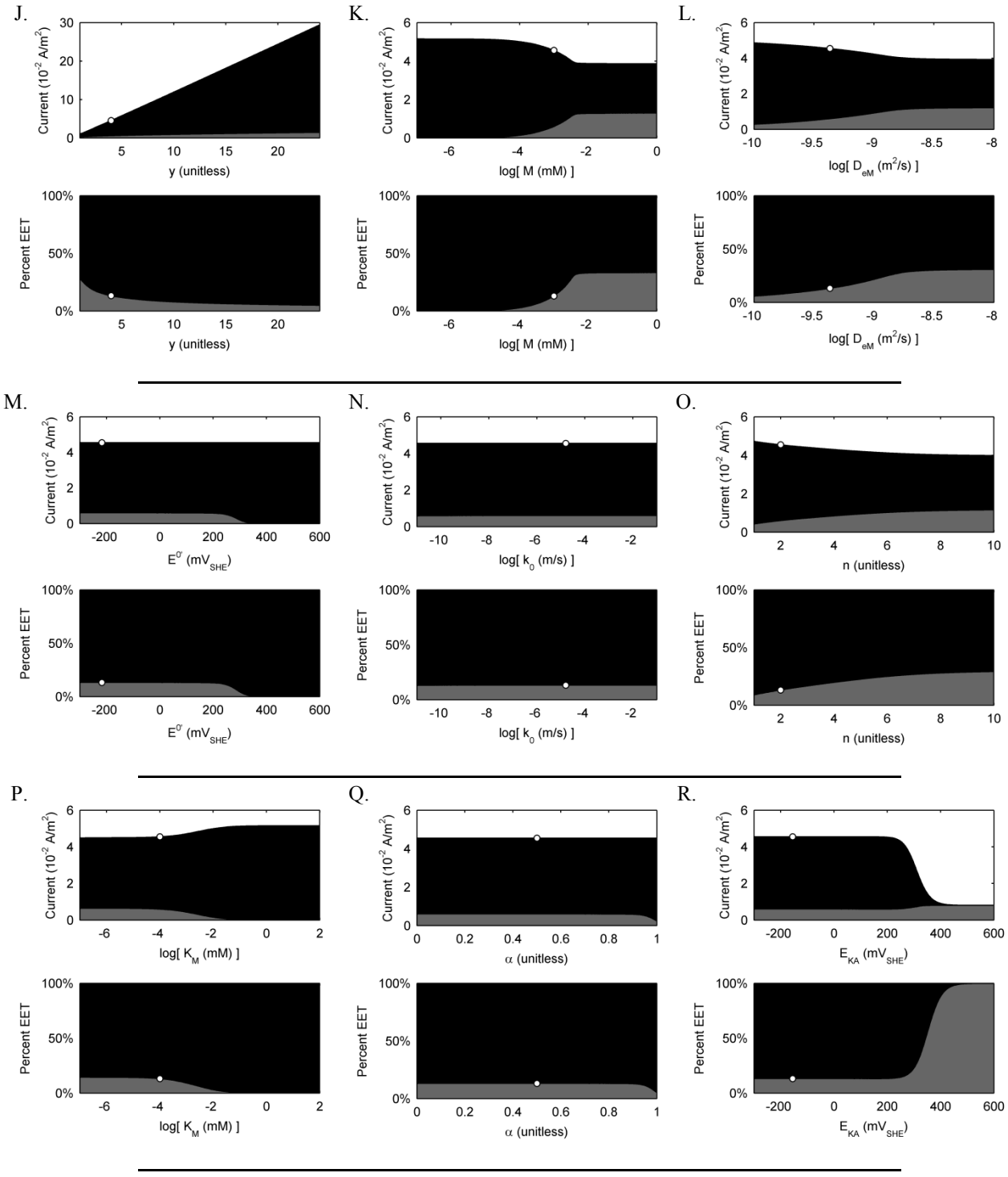
J.
K.
L.
Current (10^{-2} A/m^2)
Percent EET
y (unitless)
log[M (mM)]
log[D_{eM} (m^2/s)]
M.
N.
O.
$E^{0'}$ (mV_{SHE})
log[k_0 (m/s)]
n (unitless)
P.
Q.
R.
log[K_M (mM)]
α (unitless)
E_{KA} (mV_{SHE})

S.

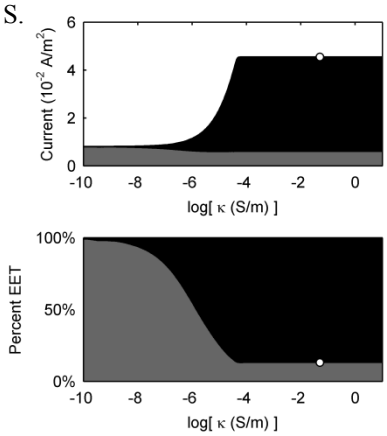

Figure S3. Parameter Analysis. Each panel (A through S) shows the effect of changing a single parameter value on anodic current production (top) and the percentage of the EET mechanism by which anodic current is generated (bottom). **Grey** represents the portion due to diffusion-based EET, and black represents the portion due to conduction-based EET. The colored areas are stacked, meaning that the interface of white and black in the current plots conveys the total current (sum of diffusion- and conduction-based EET current). Consequently, the percentage of EET total shown in each bottom plot is always 100%. The white-filled circles are provided to illustrate the parameter value and corresponding current and percent of EET for the model standard case.

The following parameter analyses are shown:

A. Polarized electrode potential ..... ε
B. Relative effective diffusion coefficient ..... D_r
C. Fraction of electrons recoverable for current ..... f
D. Biofilm thickness L
E. Maximum specific lactate utilization rate ..... q_{max}
F. Biofilm density X
G. Bulk lactate concentration ..... S
H. Effective diffusion coefficient for lactate ..... D_{eS}
I. Half-saturation constant for lactate ..... K_S
J. Electron equivalence of lactate ..... y
K. Bulk FMN concentration ..... M
L. Effective diffusion coefficient for $FMN/FMNH_2$ ..... D_{eM}
M. Standard redox potential for the $FMN/FMNH_2$ redox reaction ..... $E^{0'}$
N. Standard heterogeneous rate constant for the $FMN/FMNH_2$ redox reaction ..... k_0
O. Electrons transferred per $FMN/FMNH_2$ redox reaction ..... n
P. Half-saturation constant for FMN ..... K_M
Q. Transfer coefficient for the $FMN/FMNH_2$ redox reaction ..... α
R. Half-maximum rate potential ..... E_{KA}
S. Biofilm conductivity ..... κ

IV. VOLTAMMETRIC WAVE FORMS

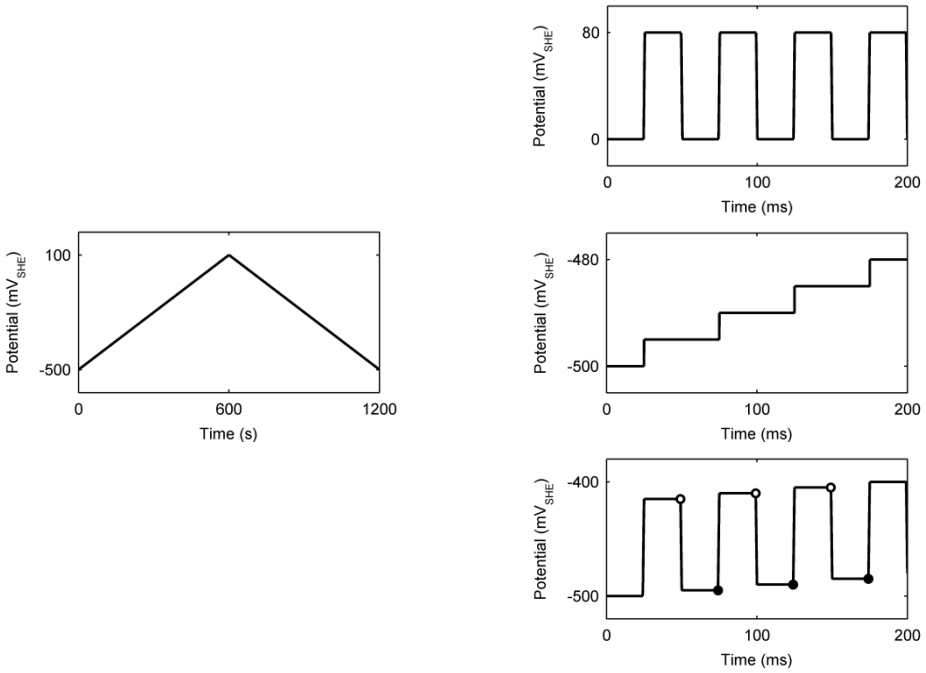

Figure S4. Wave forms for cyclic and squarewave voltammetry. Left) Cyclic voltammetry waveform with a 1-mV/s scan rate, a minimum potential of -500 mV_{SHE}, and a maximum potential of 100 mV_{SHE}. These parameters are identical to those used to generate the 1-mV/s scan rate voltammograms in the manuscript. Right) The development of the potential waveform for squarewave voltammetry. At the top is shown a squarewave potential and in the middle is shown a staircase potential. These two waveforms combined produce the final potential waveform for squarewave voltammetry, shown at the bottom. The open circles show the time when current is measured for the end of peak potential, and the filled circles show the time when current is measured for the end of trough potential. The final squarewave voltammogram is composed of the difference between the current measured at the end of the peak potential and that measured at the end of the trough potential. The waveform has a starting potential of -500 mV_{SHE}, a final potential of 100 mV_{SHE}, a potential step height of 5 mV, a pulse potential of 40 mV, and a 20-Hz scan frequency. These parameters are identical to those used to generate all squarewave voltammograms in the manuscript.

V. SUPPLEMENTARY INFORMATION FOR MODEL PARAMETERS

Table S1. Details of several anaerobic *S. oneidensis* MR-1-based MFCs with lactate as the electron donor. Coulombic efficiencies are based on the partial oxidation of lactate to acetate.

STUDY	TEMP. (°C)	LACTATE CONC. (mM)	ELECTRODE MATERIAL	COULOMBIC EFFICIENCY	
Bretschger *et al*. 2010[1]	22	5	graphite felt	54%*	
Lanthier *et al*. 2008[2]	30	10	graphite sticks	56%	
Newton *et al*. 2009[3]	25	10	graphite felt	48%*	
Watson *et al.* 2010[4]	23	18	graphite fibers	16%†	
Watson *et al.* 2010[4]	23	18	graphite paper	25%†	
Watson *et al.* 2010[4]	23	18	graphite paper	24%†	
Watson *et al.* 2010[4]	23	18	graphite brush	20%†	
Qain *et al*. 2009[5]	RT	20	gold	2.8%	micro-MFC
Rosenbaum *et al*. 2011[6]	30	20	graphite paper	11%	
Velasquez-Orta *et al*. 2010[7]	-	60	graphite plate	6%	

* Indicates coulombic efficiencies that were corrected to be based on the partial oxidation of lactate to acetate rather than on the complete oxidation of lactate to CO_2. Calculations of coulombic efficiency are described in Logan *et al*.[8]

† Values read from a figure

RT: room temperature

Table S2. Conductivities of several materials compared to the conductivity used in the standard case *Shewanella oneidensis* biofilm model.

MATERIAL	CONDUCTIVITY (mS/cm)
Silver	630,000,000
Iron	100,000,000
Graphite	20,000
Individual *S. oneidensis* nanowire[9]	1,000
This study: standard case *S. oneidensis* biofilm	0.5
Silicon	0.0156
Rubber	0.0000000000001

Reference (except where otherwise specified):
Serway, Raymond A. *Principles of Physics*. Fort Worth: Saunders College Pub., 1998.

Extended Flavin Discussion

Recently, actively secreted flavins have been identified as the electron mediators in *S. oneidensis*[7, 10, 11]. In the majority of studies, *S. oneidensis* under anaerobic conditions produces flavin mononucleotide (FMN) at the highest percent, followed by riboflavin (RF), and then by a very low percent of flavin adenine dinucleotide (FAD)[7, 11-15]. Table S3 shows a summary of the properties of each of these flavins. Because of its prevalence, FMN was chosen as the electron mediator for the standard case. Each flavin, including FMN, can undergo a two-step oxidation. When fully oxidized, or in the flavoquinone form (FMN), it can undergo a single-electron reduction to the flavosemiquinone form (FMNH) and then a second single-electron reduction to the flavohydroquinone form ($FMNH_2$). This is shown for FMN:

$$FMN + H^+ + e^- \rightleftarrows FMNH$$

Equation 1

$$FMNH + H^+ + e^- \rightleftarrows FMNH_2$$

Equation 2

It has been found that flavosemiquinones generally only exist in a low concentration (around 2%[16], although they were previously believed to be in much higher concentrations[17]), as they are rapidly converted through the fast reaction of 2 flavosemiquinones to 1 flavoquinone and 1 flavohydroquinone[18]. The full reduction of flavoquinones to flavohydroquinones is very rapid and can be considered a single two-electron reduction step as shown:

$$FMN + 2H^+ + 2e^- \rightleftarrows FMNH_2$$

Equation 3

For this model we assume that the redox reactions occur in a single two-electron transfer step, which occurs at a single redox potential. Note that rapid experiments that look at the mechanisms of each electron step report separate standard redox potentials for the flavoquinone-flavosemiquinone and flavosemiquinone-flavohydroquinone reactions for all three flavins[19]. In our model we neglect the loss of flavin mediators due to adsorption to the electrode surface. Adsorbed flavins are believed to increase the electron transfer rate of other flavins, and, in fact, flavins may only be able to transfer electrons to graphite electrodes through contact with adsorbed flavins[18]. We assume that the graphite electrode has steady state flavin coverage and that soluble flavin concentrations are not affected by adsorptive/desorptive processes. Common values for the standard redox potentials of flavins have been -208 mV vs. the standard hydrogen electrode (SHE) for riboflavin[20] and -219 mV_{SHE} for both FAD and FMN[21]. In this study, however, we chose to use values listed by Ksenzhek and Petrova[17], which have been updated to reflect more modern experiments. For all of the values in their study, we corrected the potential for temperature if it was different from 30 °C using the Nernst equilibrium equation ($nK = \frac{nFE^\circ}{RT}$), the van 't Hoff equation, and enthalpy change values for the flavin reductions given by Beaudette and Langerman[22] and Watt and Burns[23]. By averaging the values in their table, we obtain the redox potentials listed in Table S3. For the standard case simulation, the mediator (FMN) has a standard redox potential of -217 mV_{SHE}.

Table S3. Properties of the three common electron mediator flavins at 30 °C

FLAVIN	**MOLAR MASS** $g\ mol^{-1}$	**DIFFUSION COEFFICIENT** $m^2\ s^{-1}$	**STANDARD REDOX POTENTIAL** V_{SHE}
RF	376.36	$0.52 \cdot 10^{-9}$	-0.211
FMN	456.34	$0.48 \cdot 10^{-9}$	-0.217
FAD	783.53	$0.36 \cdot 10^{-9}$	-0.221

Extended Diffusion Coefficient Discussion

The diffusion coefficients of all species in this model were calculated using the Hayduk and Laudie method at 30 °C[24]. This method is based on the viscosity of the solvent and the Le Bas molar volume of the solute[25]. Calculations were performed using an online calculator[26] developed by the United States Environmental Protection Agency for modelers with methods taken from Tucker and Nelken[27]. The diffusion coefficients of riboflavin, FMN, and FAD are given in Table S3. Based on measurements by Visser and Hoek[28], Verhagen and Hagen[18] reported the diffusion coefficient of FAD at 30 °C to be $0.38 \cdot 10^{-9}$ m^2 s^{-1}, revealing that the calculated diffusion coefficient of FAD was off by 5%, which is less than the expected 18% uncertainty for the Hayduk and Laudie method[29]. The calculated diffusion coefficient of lactate is $1.22 \cdot 10^{-9}$ m^2 s^{-1}, which is only 4% off the value determined experimentally by Øyaas *et al*.[30] These results support the appropriateness and accuracy of the Hayduk and Laudie method for obtaining diffusion coefficient values for modeling.

SUPPLEMENTARY WORKS CITED

1. O. Bretschger, A. C. M. Cheung, F. Mansfeld and K. H. Nealson, *Electroanalysis*, 2010, **22**, 883-894.

2. M. Lanthier, K. B. Gregory and D. R. Lovley, *FEMS Microbiol. Lett.*, 2008, **278**, 29-35.

3. G. J. Newton, S. Mori, R. Nakamura, K. Hashimoto and K. Watanabe, *Appl. Environ. Microbiol.*, 2009, **75**, 7674-7681.

4. V. J. Watson and B. E. Logan, *Biotechnol. Bioeng.*, 2010, **105**, 489-498.

5. F. Qian, M. Baum, Q. Gu and D. E. Morse, *Lab Chip*, 2009, **9**, 3076-3081.

6. M. A. Rosenbaum, H. Y. Bar, Q. K. Beg, D. Segre, J. Booth, M. A. Cotta and L. T. Angenent, *Bioresource technology*, 2011, **102**, 2623-2628.

7. S. B. Velasquez-Orta, I. M. Head, T. P. Curtis, K. Scott, J. R. Lloyd and H. von Canstein, *Applied Microbiology and Biotechnology*, 2010, **85**, 1373-1381.

8. B. E. Logan, B. Hamelers, R. A. Rozendal, U. Schrorder, J. Keller, S. Freguia, P. Aelterman, W. Verstraete and K. Rabaey, *Environ. Sci. Technol.*, 2006, **40**, 5181-5192.

9. M. Y. El-Naggar, G. Wanger, K. M. Leung, T. D. Yuzvinsky, G. Southam, J. Yang, W. M. Lau, K. H. Nealson and Y. A. Gorby, *Proceedings of the National Academy of Sciences of the United States of America*, 2010, **107**, 18127-18131.

10. E. Marsili, D. B. Baron, I. D. Shikhare, D. Coursolle, J. A. Gralnick and D. R. Bond, *Proc. Natl. Acad. Sci. U. S. A.*, 2008, **105**, 3968-3973.

11. H. von Canstein, J. Ogawa, S. Shimizu and J. R. Lloyd, *Appl. Environ. Microbiol.*, 2008, **74**, 615-623.

12. N. J. Kotloski and J. A. Gralnick, *mBio*, 2013, **4**.

13. E. D. Brutinel and J. A. Gralnick, *Applied Microbiology and Biotechnology*, 2012, **93**, 41-48.

14. E. D. Covington, C. B. Gelbmann, N. J. Kotloski and J. A. Gralnick, *Molecular Microbiology*, 2010, **78**, 519-532.

15. H. Wang, K. Hollywood, R. M. Jarvis, J. R. Lloyd and R. Goodacre, *Appl. Environ. Microbiol.*, 2010, **76**, 6266-6276.

16. F. Müller, *Free Radical Biology and Medicine*, 1987, **3**, 215-230.

17. O. S. Ksenzhek and S. A. Petrova, *Bioelectrochemistry and Bioenergetics*, 1983, **11**, 105-127.

18. M. F. Verhagen and W. R. Hagen, *Journal of Electroanalytical Chemistry*, 1992, **334**, 339-350.

19. R. F. Anderson, *Biochimica et Biophysica Acta (BBA) - Bioenergetics*, 1983, **722**, 158-162.

20. L. Michaelis, M. P. Schubert and C. V. Smythe, *J. Biol. Chem.*, 1936, **116**, 587-607.

21. H. J. Lowe and W. M. Clark, *J. Biol. Chem.*, 1956, **221**, 983-992.

22. N. V. Beaudette and N. Langerman, *Archives of Biochemistry and Biophysics*, 1974, **161**, 125-133.

23. G. D. Watt and A. Burns, *Biochemical Journal*, 1975, **152**, 33-37.

24. W. Hayduk and H. Laudie, *AIChE Journal*, 1974, **20**, 611-615.

25. G. L. Bas, *The Molecular Volumes of Liquid Chemical Compounds from the point of view of Kopp*, Longmans, Green & Co, London, 1915.

26. EPA, EPA On-line Tools for Site Assessment Calculation: Estimated Diffusion Coefficients - Extended Chemical Range, http://www.epa.gov/athens/learn2model/part-two/onsite/estdiffusion-ext.html, Accessed December 16, 2010.

27. W. A. Tucker and L. H. Nelken, in *Handbook of chemical property estimation methods: environmental behavior of organic compounds*, eds. W. J. Lyman, D. H. Rosenblatt and W. F. Reehl, American Chemical Society, Washington, DC, 1982.

28. A. J. W. G. Visser and A. v. Hoek, *Proceedings of SPIE: Time-resolved laser spectroscopy in biochemistry*, 1988, **909**, 61-68.

29. R. H. Perry, D. W. Green and J. O. Maloney, eds., *Perry's chemical engineers' handbook*, McGraw-Hill, New York, 1997.

30. J. Øyaas, I. Storrø, H. Svendsen and D. W. Levine, *Biotechnol. Bioeng.*, 1995, **47**, 492-500.